Proc. of the Second Intl. Conf. on Advances in Civil, Structural and Construction Engineering - CSCE 2015

ISBN: 978-1-63248-042-2 doi: 10.15224/ 978-1-63248-042-2-11

Experimental and Numerical Modeling of Flow over a Spillway

[Veysel Gumus, N. Goksu Soydan, Oguz Simsek, M. Salih Kirkgoz, M. Sami Akoz]

***Abstract*—The measured velocity field and free surface profile of flow for two different discharges over a spillway model are used for validation purpose of the two-dimensional computational results of the same flow cases. The governing equations of the spillway flows are numerically solved using Finite Volume Method. The turbulence closure models; Standard k-ε, Renormalization Group k-ε, Realizable k-ε, Modified k-ω, Shear Stress Transport and Reynolds Stress Model are used in the numerical simulation and the flow profiles are computed using Volume of Fluid (VOF) method. The testing of the numerical results for grid-independent numerical solution is carried out using a GCI analysis. The comparisons of the computed and experimental results for both cases show that the numerical results from the Realizable k-ε model is more successful in predicting the velocity field and free surface of the spillway flow.**

***Keywords*—Spillway, Numerical solution, Turbulence models, Finite Volume Method, VOF**

I. Introduction

Spillway structure is used to transfer the flood water from the dam reservoir to the downstream river flow. The design of chute spillways is normally based on the principles of open channel flow. Studies related to the hydraulic design of spillways are mostly supported by the physical model tests. However, the laboratory tests may usually be costly and also time consuming. Therefore, it would be desirable to follow a calculation method which is fast, economical and safe in designing the dam spillways. It is obvious that laboratory testing through a physical model for water-structure interaction gives an important information about the specified performance criteria. In addition to the physical model studies, the numerical modeling techniques have currently made it possible to solve the flow problems economically in a short time and to repeat the design process for different conditions rapidly. However, in employing the numerical modeling for solving a flow problem, besides searching the most realistic and feasible computational fluid dynamics (CFD) technique to be applied for the numerical experimentation, the selection of an appropriate turbulence closure model is also an important question for the flow type that is under investigation.

Veysel Gumus
Harran University
Sanlıurfa

N. Goksu Soydan, Oguz Simsek, M. Salih Kirkgoz, M. Sami Akoz
Cukurova University
Adana

In this regard, the efforts to validate the numerical results with experiments and the diversification of the studies as such are needed to increase the reliability of the CFD modeling. In the past, many experimental and theoretical studies have been carried out for the analysis of spillway flows and open channel flows that interacts with different weir structures [1, 2]. Chen et. al. [3] calculated the surface profiles of the flow over a step spillway using the VOF method and compared the numerical results using the Standard k-ε turbulence model with those of experiments. From the comparisons, they reported that the calculated free surface profiles are fairly compatible with measured ones. Chatila and Tabbara [4] investigated the free surface profiles numerically over an ogee spillway for different flow conditions with ADINA software package. They stated that the numerical results obtained from the Standard k-ε turbulence closure model is consistent with the laboratory measurements. Morales et. al. [5] carried out studies on the experimental and numerical modelling of flow profile over the ogee spillway and the subsequent hydraulic jump phenomenon. They compared the numerical results for the flow profile and the length of hydraulic jump obtained from the Standard k-ω turbulence closure model with the measurements and concluded that the numerical results are compatible enough with measured values.

In this study, the experimental data for two different flow rates collected earlier from a laboratory spillway model were used for the validation of the numerical results obtained for the same conditions. The governing equations of flow interacting with the spillway model were solved with finite volume method based on ANSYS-Fluent software package. In order to obtain grid independent numerical solutions, three different concentrations of grids (coarse, medium and fine) were designed and the suitability of the fine grid was tested with Grid Convergence Index (GCI) method. Six turbulence closure models namely; Standard k-ε (SKE), Renormalization-Group k-ε (RNG), Realizable k-ε (RKE), Modified k-ω (MKW), Shear Stress Transport (SST) and Reynolds Stress Model (RSM) were used for the numerical solution of the velocity field. For the calculation of water surface profile Volume of Fluid Method (VOF) was used. The free surface profiles and velocity field obtained from the numerical simulations were compared with measured values, and the success of the chosen turbulence closure models were discussed.

II. Experiments

The free surface profile and velocity field of two-dimensional flow over a chute spillway were measured in an open channel model by Guzel [6] at Hydraulics Laboratory of Civil Engineering Department, Cukurova University. The experiments were conducted in a glass-walled, hydraulically

Proc. of the Second Intl. Conf. on Advances in Civil, Structural and Construction Engineering - CSCE 2015

ISBN: 978-1-63248-042-2 doi: 10.15224/ 978-1-63248-042-2-11

smooth, rectangular spillway channel of 0.20 m wide, 0.20 m deep and 1.80 m long.

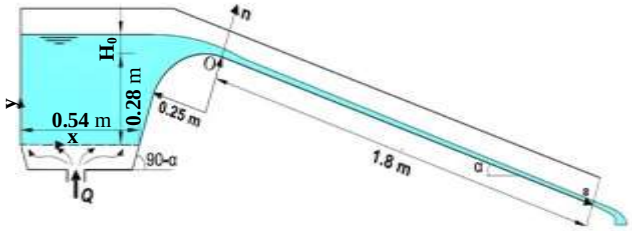

Figure 1. Experimental facility.

As may be seen in Fig. 1, x, y coordinate system for the solution domain is located at the bottom left corner. A new coordinate system (s, n) is defined for spillway flow at the beginning of the channel and H_0 is the head on the spillway. The slope angle of spillway channel is α=32°. The velocity profiles were measured at flow sections of s=0.04, 0.14, 0.24, 0.34, 0.44, 0.64, 0.74, 0.91, 1.06, 1.21, 1.36 and 1.51 m using Laser Doppler Anemometry (DISA55L). The characteristics of the two different flow cases used in the present study are given in Table I.

TABLE I. The characteristics of two different flow cases

	Q (l/s)	Fr_1	Fr_2	Re_1	Re_2
Case 1	4.67	3.68	12.64	92 400	72 900
Case 2	10.66	2.71	10.04	210 700	206 400

In the table, Q is the flow discharge, Fr_1, Re_1 and Fr_2, Re_2 are Froude number and Reynolds number at s=0.04 m and s=1.51 m respectively.

III. Formulation and Numerical Modeling

A. Basic Equations

The governing equations of the present two-dimensional turbulent flows, the Reynolds-averaged continuity and Navier-Stokes equations (RANS) for an incompressible, Newtonian fluid flow can be expressed as

$$\frac{\partial \overline{u}_i}{\partial x_i} = 0 \qquad (1)$$

$$\rho\left(\frac{\partial \overline{u}_i}{\partial t} + \overline{u}_j \frac{\partial \overline{u}_i}{\partial x_j}\right) = \rho g_i - \frac{\partial \overline{p}}{\partial x_i} + \mu \frac{\partial^2 \overline{u}_i}{\partial x_j^2} + \frac{\partial \tau_{ij}}{\partial x_j} \qquad (2)$$

In Eqs. (1) and (2), u_i is velocity component in x_i-direction, g_i is gravity, p is pressure, μ is dynamic viscosity, ρ is fluid density, t is time and τ_{ij} is turbulence stress tensor. Based on the Boussinesq eddy viscosity assumption the turbulence stresses are formulated using the linear constitutive relation:

$$\tau_{ij} = -\rho\overline{u_i' u_j'} = \mu_t\left(\frac{\partial \overline{u}_i}{\partial x_j} + \frac{\partial \overline{u}_j}{\partial x_i}\right) - \frac{2}{3}\rho k \delta_{ij} \qquad (3)$$

In Eq. (3) u_i' and u_j' are horizontal and vertical velocity fluctuations, μ_t is turbulent viscosity, k ($= \overline{u_i' u_i'}/2$) is turbulent kinetic energy and δ_{ij} is Kronecker delta.

To determine the turbulent viscosity μ_t in Eq. (3), the turbulence closure models used in this study are as follows:

1-Standard k-ε (SKE) [7],

2-Renormalization-Group k-ε (RNG) [8],

3-Realizable k-ε (RKE) [9],

4-Modified k-ω (MKW) [10],

5-Shear Stress Transport (SST) [11],

6-Reynolds Stress Model (RSM) [12].

B. Volume of Fluid (VOF) Method

The VOF method renders the shape and location of a constant-pressure free surface boundary of the flow field. It uses a filling process to determine which cell in the meshing volume is filled and which one is emptied [13]. Consider an Eulerian structured fixed grid and a curved liquid surface of a 2D flow field. A volume fraction field (F) is then defined in this grid that can take values between 0 and 1, i.e. F = 0 if the cell is emptied and F = 1 when it is completely filled with liquid. A value of F between 0 and 1 means a fractional fill with the free surface located within the cell.

C. Numerical Solution

In the numerical modeling, SIMPLE (Semi-implicit method for pressure-linked equations) algorithm was used for velocity-pressure coupling which is designed specifically for transient simulations [14]. First-order upwind discretization scheme was used for the momentum, turbulent kinetic energy and dissipation equations; and in the discretization of pressure term PRESTO (Pressure staggered option) algorithm was employed [15]. In the computations, the residual error as a convergence criterion was within 10^{-4} for all the computed variables (u, v, k, ε).

In the computations, it is necessary to keep the simulation throughout stable due to the demands of the VOF model. At each time step, the maximum iteration number was 10. The computations for the present cases showed that for the establishment of a stable flow field, a time span of the order of 30 s is required. That means nearly 76,000 time steps are needed to reach steady-state conditions.

The numerical solution of governing equations (2) and (3) for the variables, $\overline{u}$, $\overline{v}$ and $\overline{p}$, was carried out using ANSYS-Fluent v.12.1 program package which is based on the finite volume method [16].

Proc. of the Second Intl. Conf. on Advances in Civil, Structural and Construction Engineering - CSCE 2015

ISBN: 978-1-63248-042-2 doi: 10.15224/ 978-1-63248-042-2-11

D. Solution Domain, Boundary and Initial Conditions

The geometry of the two-dimensional solution domain and the boundary conditions are shown in Fig. 2. At the air-filled upper boundary of the solution domain, the pressure p =0. At the inlet boundary, the flow velocities were v = 0.0432 m/s and 0.0987 m/s, and u =0 for Case 1 and Case 2, respectively. The outlet boundary was a free over fall at the outlet boundary where p = 0. All of the wall boundaries were set as stationary, i.e. non-slip wall. The viscosity dominated near-wall region was dealt with the enhanced two-layer wall treatment.

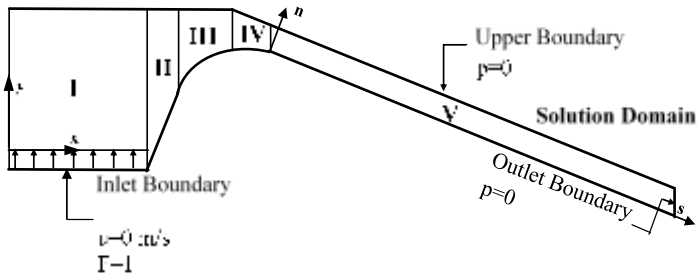

Figure 2. Geometry and boundary conditions of solution domain.

IV. Computational Grid

The resolution of the computational discretization of the solution domain is important for an ultimate grid-independent solution. For the purpose of designing a suitably-spaced computational grid system, structured grids of different local cell concentrations were tested [17,18]. Considering the flow characteristics for the present interaction problem, the solution domain was divided into five regional sub-domains. Due to the increasing velocity gradient, the density of discretization was intentionally increased towards the solid boundary by compressing the grid system. Three grid systems with different density, Grid 1 (coarse), Grid 2 (medium) and Grid 3 (fine), were used to examine the effect of the grid size on the accuracy of the numerical results. The element numbers of the three computational grids is summarized in Table II. Fine grid which is adopted for the final design of the computational grid system, containing eleven sub-domains, is seen in Fig. 3.

Table III gives the GCI values for selected channel sections. It is seen from the table that the predicted errors in the flow velocity due to discretization for the fine-grid solutions were found within 2% which is well acceptable for the verification of computed results.

TABLE II. Sub-domain element numbers of computational grids for three different densities

Region	Coarse	Medium	Fine
I	40x75	60x100	80x150
II	15x75	20x100	30x150
III	30x75	45x100	60x150
IV	25x75	35x100	50x150
V	200x75	300x100	400x150

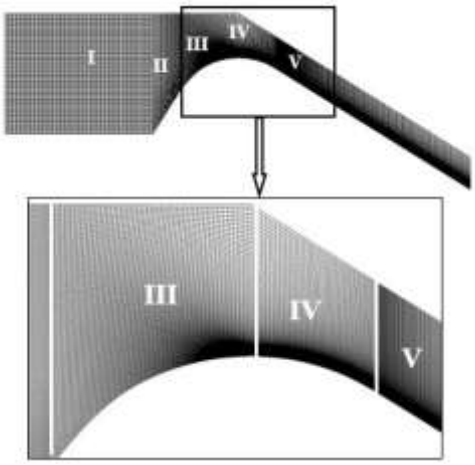

Figure 3. Sub-domains of computational grid

TABLE III. GCI values for selected sections

n (mm)	s=0.24 m	0.74	1.21	1.51
0.3	0.0512	0.8115	0.2971	0.0429
0.5	0.0351	-1.2459	-1.6895	-1.9090
0.8	0.0411	-1.3256	-1.3446	0.2962
1.0	0.1156	-1.5689	-1.0235	0.0190
2.0	-0.4497	1.6845	-1.0118	-0.6074
3.0	-0.2642	0.7323	1.3569	-1.3125
4.0	-01761	0.7325	1.6598	-1.4569
8.0	0.0005	0.6355	1.1252	-1.6581
10.0	0.0003	0.0588	-1.4587	-1.8457
12.0	0.0001	0.0052	-0.2324	-1.4129

V. Results

In the comparisons of computed velocity profiles from different turbulence closure models with those of experiments, mean square error (MSE) values were used as a quantitative evaluation criterion. MSE of measured and predicted velocity profiles in the channel is expressed as

$$\mathrm{MSE} = \frac{1}{N}\sum_{n=1}^{N}(v_m - v_p)^2 \qquad (4)$$

where v_m and v_p are measured and predicted velocity values, respectively, along the solution domain and N is the total number of velocities in the flow profile.

The results of MSE values calculated for the velocity profiles from the different turbulence closure models for both cases are given in Table IV and Table V. The numbers as superscript on MSE values indicate the order of success in regard to compliance with the experimental measurements. The mean MSE results in the table indicates that the computational results for the velocity profiles by using RKE turbulence closure model is better than those predicted by other models for both flow cases tested. It can also be said that MKW turbulence model produces the poorest predicted results compared to the other models used in this study.

Proc. of the Second Intl. Conf. on Advances in Civil, Structural and Construction Engineering - CSCE 2015

ISBN: 978-1-63248-042-2 doi: 10.15224/ 978-1-63248-042-2-11

TABLE IV. MSE statistics for different turbulence closure models (Case 1)

s (m)	MSE (cm^2/s^2)					
	SKE	RNG	RKE	MKW	SST	RSM
0.04	7.469[5]	**4.654[1]**	4.728[2]	13.027[6]	5.197[3]	5.462[4]
0.14	2.747[5]	**1.404[1]**	1.423[2]	7.389[6]	1.631[3]	2.340[4]
0.24	3.055[5]	1.678[3]	**1.617[1]**	8.092[6]	1.648[2]	2.948[4]
0.34	5.727[5]	2.940[3]	2.881[2]	13.769[6]	**2.258[1]**	4.206[4]
0.44	6.051[5]	3.579[3]	3.547[2]	15.503[6]	**2.702[1]**	5.651[4]
0.64	7.806[4]	4.840[2]	4.961[3]	21.417[6]	**3.938[1]**	8.152[5]
0.74	16.860[5]	8.623[3]	8.058[2]	38.051[6]	**5.026[1]**	9.392[4]
0.91	9.912[5]	5.873[3]	**5.442[1]**	25.944[6]	5.821[2]	5.976[4]
1.06	9.334[4]	7.291[3]	7.104[2]	21.670[6]	9.420[5]	**6.022[1]**
1.21	12.520[5]	10.308[3]	10.000[2]	24.813[6]	12.055[4]	**9.173[1]**
1.36	12.908[2]	12.988[3]	13.340[4]	20.024[6]	15.626[5]	**9.164[1]**
1.51	11.306[3]	11.683[4]	11.847[5]	11.190[2]	14.046[6]	**10.673[1]**
Mean	8.808[5]	6.322[2]	**6.246[1]**	18.407[6]	6.614[4]	6.597[3]

TABLE V. MSE statistics for different turbulence closure models (Case 2)

s (m)	MSE (cm^2/s^2)					
	SKE	RNG	RKE	MKW	SST	RSM
0.04	2.978[5]	1.215[2]	**0.995[1]**	3.005[6]	1.483[3]	1.523[4]
0.14	2.147[5]	0.947[2]	**0.871[1]**	11.916[6]	1.332[3]	1.796[4]
0.24	2.907[5]	0.887[2]	**0.841[1]**	18.741[6]	1.176[3]	2.074[4]
0.34	3.730[5]	1.269[3]	1.232[2]	23.324[6]	**1.186[1]**	2.569[4]
0.44	3.877[5]	1.334[3]	1.300[2]	25.895[6]	**0.923[1]**	2.284[4]
0.64	5.358[4]	3.215[2]	3.309[3]	35.945[6]	**2.281[1]**	4.902[4]
0.74	6.454[5]	3.159[2]	3.706[3]	42.397[6]	**2.310[1]**	5.585[4]
0.91	8.581[5]	2.818[3]	2.733[2]	52.360[6]	**2.574[1]**	3.532[4]
1.06	9.953[5]	2.999[3]	2.935[2]	68.397[6]	**2.896[1]**	3.406[4]
1.21	12.613[5]	3.413[3]	**3.246[1]**	84.550[6]	3.314[2]	3.774[4]
1.36	11.352[2]	5.217[3]	5.017[2]	88.274[6]	6.344[4]	**3.042[1]**
1.51	16.099[3]	9.552[3]	9.210[2]	110.749[6]	11.766[4]	**4.794[1]**
Mean	7.171[5]	3.002[2]	**2.950[1]**	47.129[6]	3.132[3]	3.273[4]

A. Velocity Profiles

The measured and predicted velocity profiles in s direction belonging to different selected sections of the chute channel are given in Figures 4 and 5 for Case 1 and Case 2. For the sake of clarity, the numerical results obtained from the three turbulence models, RKE, MKW and RSM are only included in the figures. In Figures 4 and 5 for both flow cases, the differences between the best and worst predicted velocity profiles from the RKE and MKW turbulence models can be clearly seen. RKE model shows reasonably good performance in predicting the velocity field in the boundary layer as well as outside the boundary region of the supercritical spillway flow.

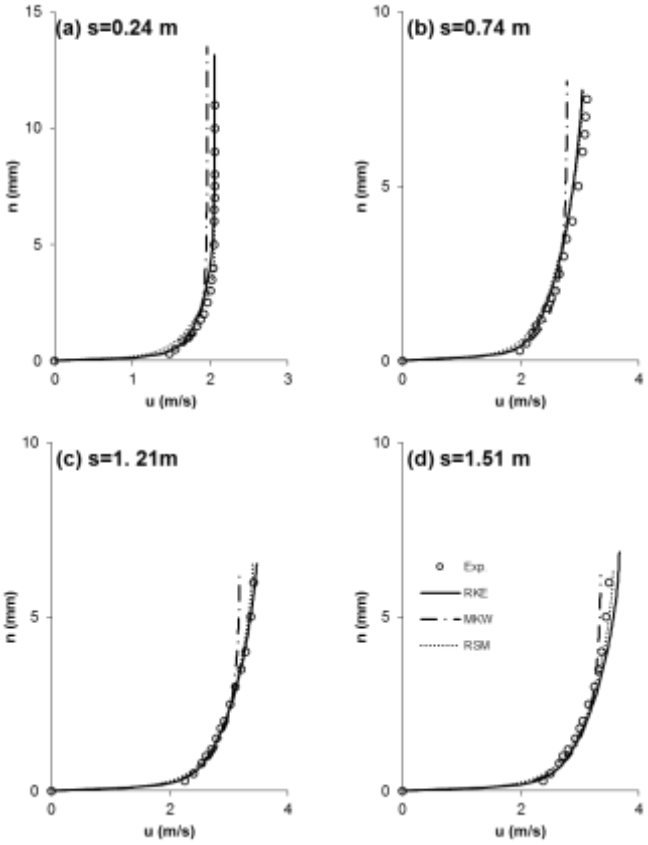

Figure 4. Experimental and computed velocity profiles for Case 1

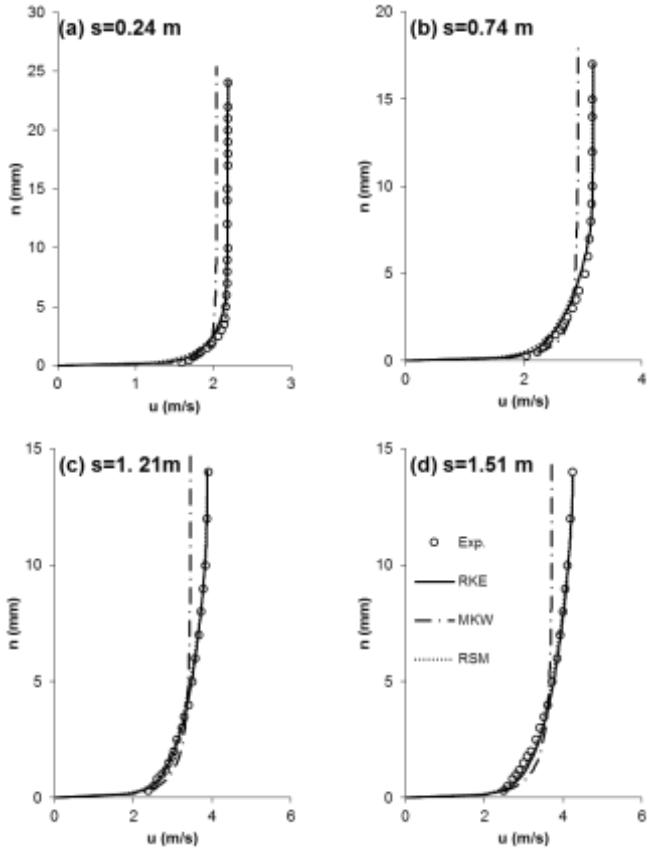

Figure 5. Experimental and computed velocity profiles for Case 2

B. Free Surface Profiles

Volume of Fluid (VOF) method is used for the determination of free surface profiles in the chute channel. Figures 6 and 7 give the experimental and computed free surface profiles obtained from RKE, MKW and RSM turbulence models that include the best and the worst predicted velocity profiles based on the MSE criterion. It is seen in Figures 6 and 7 that the predictions of gradually varied non-uniform flow profile along the chute channel by the three turbulence models are reasonably well. However, with a close inspection of the figures, it is seen that the agreement between

Proc. of the Second Intl. Conf. on Advances in Civil, Structural and Construction Engineering - CSCE 2015

ISBN: 978-1-63248-042-2 doi: 10.15224/ 978-1-63248-042-2-11

the computed and measured profiles appears to be the best for the RKE turbulence model.

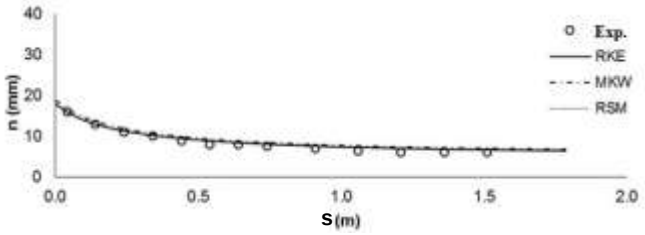

Figure 6. Experimental and computed free surface profiles for Case 1

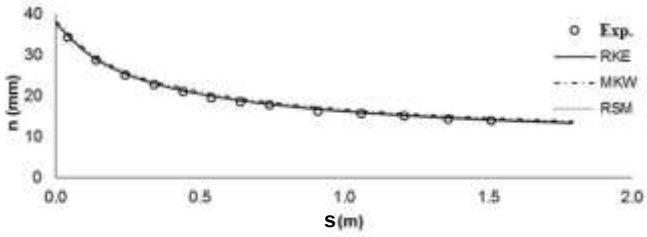

Figure 7. Experimental and computed free surface profiles for Case 2

VI. Conclusions

The experimental findings of the two different flow rates obtained from the spillway model in a laboratory were used to validate the numerical results based on the CFD analyses for the same conditions. Using the Standard k-ε, Renormalization-Group k-ε, Realizable k-ε, Modified k-ω, Shear Stress Transport and Reynolds Stress Model, the governing equations of the flow were solved by the Finite Volume Method. Computed free surface profiles and velocity profiles were compared with those obtained from the model experiments. The MSE statistics of the velocity profiles were used as a criterion for the quantitative analysis of results obtained from the turbulence closure models. Comparison of the numerical results with experiments reveals that the RKE turbulence closure model that includes parameter η, depends on the mean strain-rate tensor S_{ij}, was the most successful in predicting the velocity field and the profile of the chute flow among the six turbulence closure models employed herein.

Acknowledgment

This study was supported by the Scientific Research Projects Committee of Cukurova University with Project Number MMF2001D3.

References

[1] M. S. Kirkgoz, M. S. Akoz and A. A. Oner, "Numerical Modeling of Flow over a Chute Spillway", Journal of Hydraulic Research, 2009, vol.47(6), pp.790-797.

[2] M. S. Akoz, V. Gumus and M. S. Kirkgoz, "Numerical Simulation of Flow over a Semicylinder Weir", Journal of Irrigation and Drainage Engineering, 2014, vol. 140,6.

[3] Q. Chen, G. Q. Dai and H. W. Liu, "Volume of Fluid Model for Turbulence Numerical Simulation of Stepped Spillway Overflow", Journal of Hydraulic Engineering-Asce, 2002,vol.128(7), pp. 683-688.

[4] J. Chatila and M. Tabbara, "Computational Modeling of Flow over an Ogee Spillway", Computers & Structures, 2004, vol. 82(22), pp.1805-1812.

[5] V. Morales, T. E. Toktay and M. Garcia, "Numerical Modeling of Ogee Crest Spillway and Tainter Gate Structure of a Diversion Dam on Canar River", XIX International Conference on Water Resources Ecuador, 2012.

[6] H. Güzel, "Investigation of Energy Loss in a ;Dam Spillway Channel", MSc Thesis (In Turkish) , Cukurova University, Turkey-Adana, 1991.

[7] B. E. Launder and D. B. Spalding, Lectures in Mathematical Models of Turbulence, Academic Press, New York, 1972.

[8] V. Yakhot, S. A. Orszag, S. Thangam, T. B. Gatski and C. G. Speziale, "Development of Turbulence Models for Shear Flows by a Double Expansion Technique", Physics of Fluids a-Fluid Dynamics, 1992, vol. 4(7), pp. 1510-1520.

[9] T. H. Shih, W. W. Liou, A. Shabbir, Z. Yang and J. ZhU, "A New K-ϵ Eddy Viscosity Model for High Reynolds Number Turbulent Flows", Computers & Fluids,1995, vol. 24(3),pp. 227-238.

[10] F. R. Menter, "2-Equation Eddy-Viscosity Turbulence Models for Engineering Applications", Aiaa Journal, 1994, vol. 32(8), pp. 1598-1605.

[11] M. M. Gibson and B. E. Launder, "Ground Effects on Pressure Fluctuations in the Atmospheric Boundary Layer", J. Fluid Mech., 1978, vol 86, pp.491-511.

[12] B. E. Launder,"2nd-Moment Closure and Its Use in Modeling Turbulent Industrial Flows", International Journal for Numerical Methods in Fluids, 1989, vol. 9(8), pp. 963-985.

[13] C. W. Hirt and B. D. Nichols, "Volume of Fluid (Vof) Method for the Dynamics of Free Boundaries", Journal of Computational Physics, 1981, vol. 39(1),pp. 201-225.

[14] S. V. Patankar and D. B. Spalding, "A Calculation Procedure for Heat, Mass and Momentum Transfer in Three-Dimensional Parabolic Flows", International Journal of Heat and Mass Transfer, 1972, vol. 15(10), pp. 1787-1806.

[15] S. Patankar, "Numerical heat transfer and fluid flow", CRC Press, (1980).

[16] ANSYS Inc. (2009). Release 10.0. www.ansys.com

[17] P. J. Roache, "Verification of Codes and Calculations", Aiaa Journal, 1998, vol. 36(5), pp. 696-702.

[18] I. B. Celik, U. Ghia, P. J. Roache and C. J. Freitas, "Procedure for Estimation and Reporting of Uncertainty Due to Discretization in CFD Applications", Journal of Fluids Engineering-Transactions of the ASME, 2008, vol. 130(7).